RESEARCH ARTICLE | DECEMBER 18 2019

Non-linear behavior of flexoelectricity

Zhiguo Wang; Ruobing Song; Zhenjiang Shen; Wenbin Huang ; Chunchun Li; Shanming Ke ; Longlong Shu

Appl. Phys. Lett. 115, 252905 (2019)
https://doi.org/10.1063/1.5126987

Applied Physics Letters ARTICLE scitation.org/journal/apl

Non-linear behavior of flexoelectricity

Cite as: Appl. Phys. Lett. **115**, 252905 (2019); doi: 10.1063/1.5126987
Submitted: 7 September 2019 · Accepted: 15 November 2019 ·
Published Online: 18 December 2019

View Online Export Citation CrossMark

Zhiguo Wang,[1,a)] Ruobing Song,[2,a)] Zhenjiang Shen,[3] Wenbin Huang,[1,b)] Chunchun Li,[4] Shanming Ke,[4] and Longlong Shu[4,b)]

AFFILIATIONS

[1]The State Key Lab of Mechanical Transmissions, Chongqing University, Chongqing 400044, People's Republic of China
[2]Department of Applied Physics, The Hong Kong Polytechnic University, Kowloon, Hong Kong
[3]College of Physics and Electronic Engineering, Hainan Normal University, Haikou 571158, People's Republic of China
[4]School of Materials Science and Engineering, Nanchang University, Nanchang 330031, People's Republic of China

[a)]**Contributions:** Z. Wang and R. Song contributed equally to this work.
[b)]**Authors to whom correspondence should be addressed:** whuang@cqu.edu.cn and llshu@ncu.edu.cn

ABSTRACT

Coupling between polarization and the strain gradient, namely, flexoelectricity, is a universal phenomenon that widely exists in all solid dielectrics and polymers. At a low level of the applied strain gradient, this electromechanical coupling is strictly a linear effect. In this Letter, a strong nonlinearity between the polarization and the strain gradient was experimentally found in polyvinylidene fluoride when the strain gradient was higher than a material-dependent threshold value. Such nonlinear behavior was in good accordance with an ion chain theory and could be fitted by a nonlinear equation. The observed flexoelectric nonlinearity in this work will help in the understanding of the discrepancy between the previous findings about the bulk materials and their nanoscale counterparts.

The coupling between the electric polarization and the strain gradient, also named flexoelectricity, has become increasingly important in the cutting edge of functional materials.[1–13] This electromechanical effect was generally regarded as a linear effect and can be written in the form of

$$P = \mu \frac{\partial S}{\partial x}, \tag{1}$$

where P is the electric polarization, μ is the flexoelectric coefficient, a fourth rank tensor, and $\frac{\partial S}{\partial x}$ is the strain gradient, in a prerequisite that the strain S is inhomogeneously distributed along the x direction. In contrast to piezoelectricity, flexoelectricity is not limited to centrosymmetric materials; thus, strain gradient (not the uniform strain) induced electric polarization can exist in materials with high symmetrical crystalline structures such as cubic and isotropic structures.[14–20] Besides the broad selection of material, flexoelectricity shows an attractive size effect, whereby the flexoelectric response will be dramatically enhanced when the material dimension is reduced to the nanoscale.[21–24] This is attributed to the large strain gradient allowable at nanoscale sizes. For example, a large out-of-plane strain gradient (10^7 m^{-1}) along the thickness direction can be generated in the heterostructure thin film, resulting in a giant flexoelectric polarization comparable to or even higher than the ferroelectric/piezoelectric polarization.[6,10,25] The recently reported flexoelectricity in nanostructures and related systems clearly suggests the great potential of flexoelectricity in various applications including sensing and actuating, polarization switching, defect formation, electronic transportation, and domain engineering.[7,26–36] Though turning into the nanoscale greatly benefits the application of flexoelectricity, it will also bring several limitations. One thing that must be underlined is that for the same kind of material, the flexoelectric coefficients on the nanoscale are usually orders of magnitude smaller than their bulk counterparts, which only withstand a strain gradient at the level of 0.1 m^{-1}.[37–39] Taking the widely studied $BaTiO_3$ as an example, according to the literature, the flexoelectric coefficient in the $BaTiO_3$ ceramic was as high as 50 μC/m, while the flexoelectric coefficient in the $BaTiO_3$ thin film was less than 1 nC/m based on the back calculation of the experimental results.[6] Similar phenomena were also found in other material systems such as $SrTiO_3$ and (Ba, Sr)TiO_3 (BST),[40,41] but the mechanism for these discrepancies remains unclear.

A reasonable thought for resolving this problem is to resort to the nonlinearity of the flexoelectricity. Actually, the nonlinear behavior is a widely existing phenomenon in dielectric materials, e.g., the dielectric constant vs the electric field, the piezoelectric coefficients vs stress, the ferroelectric polarization vs the electric field, etc. The nonlinear contribution is commonly described as a high order term, which is much less significant compared to the linear part when the variable is

small. Recently, such a consideration has also been introduced for the investigation of flexoelectricity by Chu and Yang.[42] They demonstrated the quadratic flexoelectric effect in noncentrosymmetric systems via the analytical derivation of the electromechanical properties in a two-dimensional ionic chain model. However, the validity of this theory only applies for a small strain gradient scenario because the nonlinear high order term will soar up as the strain gradient increases by orders, contradicting with the declining nature of the flexoelectricity. Therefore, there should be another mechanism that leads to the unique performance of flexoelectricity at different levels of strain gradient input. In the present paper, we propose a possible explanation for the controversies of the flexoelectric coefficients on the nanoscale and macroscale by establishing an ionic chain model for simulation. Based on this finding, an inversely dependent relationship between the effective flexoelectric coefficients with the strain gradient was proposed. In order to achieve a large strain gradient, the typical soft material polyvinylidene fluoride (PVDF) was selected for the nonlinear study, while two hard materials, 0.5 wt. % Al_2O_3-doped $Ba(Ti_{0.85}Sn_{0.15})O_3$ ceramic (hereafter abbreviated as BTS) and $0.3Pb(In_{1/2}Nb_{1/2})O_3$-$0.35Pb(Mg_{1/3}Nb_{2/3})O_3$-$0.35PbTiO_3$ single crystal (hereafter abbreviated as PIN-PMN-PT), were selected as the counterparts. The experimental results correspond well with the simulation and disclose that the nonlinear contribution of the flexoelectricity will become more and more significant as the strain gradient gradually increases. The present work is believed to be able to bridge the gap between the flexoelectricity on the macroscale and nanoscale.

To investigate the flexoelectric nonlinearity, we start from the two-dimensional ionic chain model of the centrosymmetric material. The positive and negative ions have an alternative distribution with an equidistance of a under no external perturbations, as shown in Fig. 1(a). A unit cell with a central negative charge and surrounding positive charges is selected as the research object. When a strain gradient $\partial S_y/\partial x$ is generated, the negative charge is squeezed away from its original position relative to the positive charge, resulting in the dipole moment, depicted in Fig. 1(b). The internal interaction within the unit cell can be simplified as massless springs between points masses with the electric charges of $\pm q$, as shown in Fig. 1(c). Springs between the positive charges are k_x and k_y along the x and y axes, respectively. The springs connecting the positive and negative charges are denoted as k_q and k_p along the diagonals. The strain gradient of the selected lattice can be expressed as

$$\frac{\partial S}{\partial x} = \frac{u_1 - u_2}{a^2}, \tag{2}$$

where u_1 and u_2 are the relative displacement between the positive charges at the top and bottom, respectively. The forces on the negative charge from the diagonal springs are F_1 and F_2 and can be expressed as

$$\begin{aligned} F_1 &= k_q\left(\frac{a+u_1}{2\sin\theta_1} - \frac{a}{2\sin\theta}\right), \\ F_2 &= k_p\left(\frac{a+u_2}{2\sin\theta_2} - \frac{a}{2\sin\theta}\right), \end{aligned} \tag{3}$$

where $\theta = \frac{\pi}{4}$ and θ_1, θ_2 can be obtained by the following equation:

$$\begin{aligned} \tan\theta_1 &= \frac{a+u_1}{a-2u}, \\ \tan\theta_2 &= \frac{a+u_2}{a+2u}. \end{aligned} \tag{4}$$

The components of F_1 and F_2 in the vertical direction should be balanced,

$$F_1\cos\theta_1 = F_2\cos\theta_2. \tag{5}$$

Because of the discrete translational symmetry, the induced dipole moment per unit lattices p_l is written as

$$p_l = -qu, \tag{6}$$

where u is the displacement of the negative ion.

Combining these equations, the relationship between the displacement u_1 and u could be obtained when equaling u_2 to 0 and assuming $k_q = k_p$. Therefore, the relationship between the polarization and the strain gradient could be solved by the following equation:

$$\begin{aligned} &\frac{(1-2\hat{u})^2\left[1-16\hat{u}^2(1+2\hat{u}+2\hat{u}^2)+4\sqrt{2}\hat{u}(1+2\hat{u})\sqrt{1+(1+2\hat{u})^2}\right]}{(1+2\hat{u})^2(1+8\hat{u}^2)+8\hat{u}^2-4\sqrt{2}\hat{u}(1+2\hat{u})\sqrt{1+(1+2\hat{u})^2}} \\ &= (1+\hat{u}_1)^2, \end{aligned} \tag{7}$$

where $\hat{u} = \frac{u}{a}$ and $\hat{u}_1 = \frac{u_1}{a}$.

Therefore, the relationship between the dipole moment and the strain gradient was obtained by the Matlab calculation, as shown in Fig. 1(d). It can be seen that when the strain gradient is small, the polarization shows a quasilinear trend. However, the increase in dipole moment will be smaller and smaller with the increase in the strain gradient and gradually saturates to a certain level, corresponding to a strong nonlinear phenomenon. It was noticed that the ion chain model can work in different material structures. Taking the α-phase and β-phase of PVDF as examples, we can find that both the paraelectric phase and the ferroelectric phase show a similar flexoelectric nonlinearity (see the detailed calculation in the supplementary material).

Based on the above analysis, we propose a logarithmic relationship between the strain gradient and polarization,

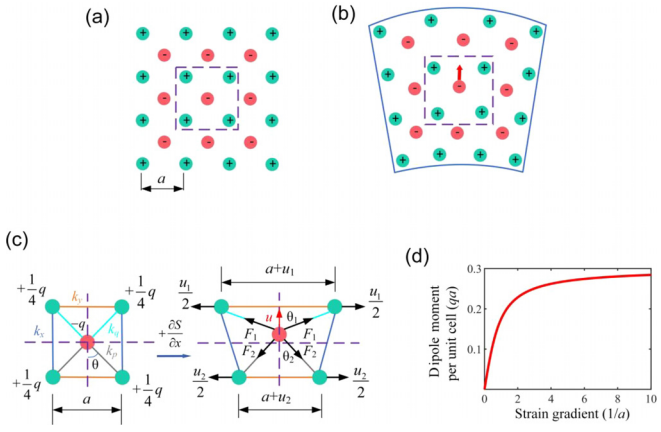

FIG. 1. (a) Two-dimensional ionic arrangement. (b) The strain gradient induced polarization. (c) A unit cell of the ionic chain model. (d) The relationship between the dipole moment and the strain gradient.

$$P = \alpha \ln\left(1 + \beta \frac{\partial S}{\partial x}\right), \tag{8}$$

where α and β are two parameters that fully describe the nonlinear property of the flexoelectricity.

Then, expanding Eq. (8) out using Taylor's formula at $\frac{\partial S}{\partial x} = 0$ yields

$$P = \alpha\beta \frac{\partial S}{\partial x} - \alpha\beta^2 \left(\frac{\partial S}{\partial x}\right)^2 + \cdots\cdots. \tag{9}$$

The higher order terms are ignored at the low strain gradient level (the value depends on β), and Eq. (9) turns into

$$P = \alpha\beta \frac{\partial S}{\partial x}. \tag{10}$$

This equation indicates that a linear performance of the flexoelectricity at the low strain gradient level and the effective flexoelectric coefficient reach a constant value, which equals $\alpha\beta$, being consistent with the linearity obtained in the bulk.

In addition, the effect of the nonlinear term (higher order terms) plays a larger role as the strain gradient increases. It can be seen that the crossover of nonlinear and linear terms occurs at a strain gradient $\frac{\partial S}{\partial x} = \frac{1}{\beta}$ in Eq. (9), which means that the value of the nonlinear term will exceed the linear one when $\frac{\partial S}{\partial x} > \frac{1}{\beta}$. Therefore, $\frac{1}{\beta}$ can also be regarded as the critical threshold value of the strain gradient, which is responsible for flexoelectric nonlinearity.

However, Taylor's formula no longer works as the strain gradient becomes orders of magnitude higher (e.g., 10^6–10^7 m^{-1}). The derivative of polarization with respect to the strain gradient could yield the effective flexoelectric coefficient, given as

$$\mu_{eff} = \frac{\partial P}{\partial\left(\frac{\partial S}{\partial x}\right)} = \frac{\alpha\beta}{1 + \beta \frac{\partial S}{\partial x}}. \tag{11}$$

The limit of the effective flexoelectric coefficient at the high strain gradient level can be obtained as

$$\lim_{\partial S/\partial x \to \infty} \mu_{eff} = \alpha/(\partial S/\partial x). \tag{12}$$

It can be seen that the effective flexoelectric coefficient will decrease rapidly, showing a conversely dependent relationship with the strain gradient.

It is noticed that, in some scenarios such as crack, the nonlinearity of flexoelectric coefficients becomes extremely important. This is because the highest strain gradient the material can withstand occurs in the vicinity of crack.[43] In this scenario, the nonlinear part of the flexoelectric polarization will far exceed the linear part. Therefore, the electric polarization around crack was mainly determined by the flexoelectric nonlinearity.

To verify the effectiveness of the proposed model for describing the nonlinear flexoelectricity, three typical materials including the BTS ceramic, PIN-PMN-PT single crystal, and PVDF polymer were selected in the bulk cantilever configuration, with the experimental setup shown in Fig. 2(a). Large strain gradients approaching the breaking limit of the material were applied upon the cantilever to achieve a significant nonlinear effect.

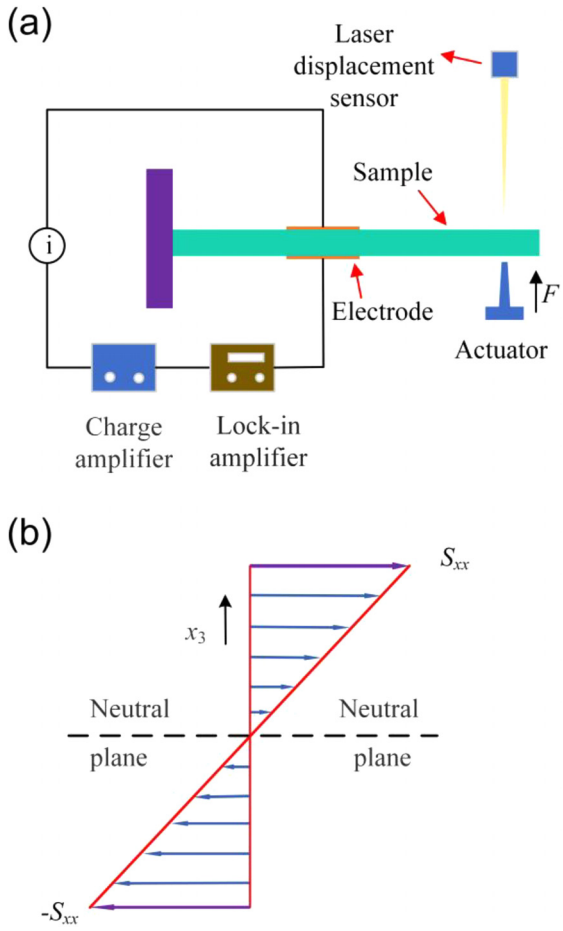

FIG. 2. (a) The schematic view of the nonlinear flexoelectric measurement of the BTS ceramic and PIN-PMN-PT single crystal. (b) The linear normal strain distribution of the beam along the thickness direction.

Due to the fragile nature of the BTS ceramic and PIN-PMN-PT single crystal, a piezoelectric stack actuator with the precise deformation control capability was employed to drive the cantilever samples. The cantilevers were fixed at one end while driven by the actuator at the other end. In order to obtain the quasistatic vibration of the cantilever, a 7 Hz sinusoidal signal was applied using a function generator. The displacement can be measured using a laser displacement sensor (KEYENCE, LK-G80), and the strain gradient can be calculated using the geometric parameters. The charge output on the sample electrode was collected using a charge amplifier (SINOCERA, YE5852) connected to a lock-in amplifier (STANFORD RESEARCH SYSTEMS, SR830).

The plane section assumption is used in the calculation of the strain gradient of materials in the case of a slender beam with pure bending. A linearly distributed normal strain S_{xx} along the thickness of the material is produced with a zero strain at the neutral plane. The upper part of the material is subjected to the compressive stress, and the strain of the upper surface is S^s_{xx}. On the contrary, the lower part is subjected to tensile stress, and the strain of the lower surface is $-S^s_{xx}$ [Fig. 2(b)].

The strain gradient along the thickness direction equals the curvature κ, which can be expressed as a function of the deflection $w(x)$,

$$\kappa = \frac{\frac{d^2w(x)}{dx^2}}{\left[1+\left(\frac{dw(x)}{dx}\right)^2\right]^{3/2}} = \frac{\partial S_{11}}{\partial x_3}. \tag{13}$$

In the case of small deformation, the value of $\frac{dw(x)}{dx}$ is much less than 1 and Eq. (13) can be simplified as

$$\kappa = \frac{d^2w(x)}{dx^2}. \tag{14}$$

Through the integral and the boundary conditions of the cantilever beam, the deformation $w(x)$ can be calculated as

$$w(x) = \frac{3w(L)}{2L^2}\left(1-\frac{x}{3L}\right)x^2. \tag{15}$$

Hence, the strain gradient can be derived as

$$\frac{\partial S_{11}}{\partial x_3} = \frac{3w(L)}{L^2}\left(1-\frac{x}{L}\right). \tag{16}$$

The polarization can be obtained by the total electric charge collected on the electrode,

$$P = \frac{Q}{A}, \tag{17}$$

where A is the electrode area.

In terms of the PVDF polymer, a larger strain gradient can be induced through a larger deflection. However, in the case of large deformation, $\frac{dw(x)}{dx}$ cannot be omitted in Eq. (13), which brings difficulties to the calculation of the strain gradient. In this paper, the difficult calculation of the strain gradient is avoided by measuring material surface strain through a strain gauge.

To yield a large strain gradient, the geometry of PVDF samples was specially designed where the length exceeds 100 mm, as shown in Fig. 3(a). The nonlinear flexoelectricity in PVDF was measured using a modulated cantilever system shown in Fig. 3(b). A shaker (HEV-200) driven by a power amplifier (HEV-200C) was used to drive the cantilever sample to provide a large displacement. In order to obtain the quasistatic vibration of the cantilever, a 7 Hz sinusoidal signal was applied by the function generator. The strains on the surface of the sample were measured by the strain gauge, and the strain gradient can be calculated by assuming a linear strain distribution along the thickness direction. In the same way, the charge output on the sample electrode was collected by a charge amplifier connected to a lock-in amplifier. The thickness of material is h, and thus, the strain gradient can be obtained as

$$\frac{\partial S_{11}}{\partial x_3} = \frac{2S^s_{xx}}{h}. \tag{18}$$

The PVDF polymer was examined using an X-ray diffractometer with Cu Kα radiation ($\lambda = 0.15406$ nm) operating at 40 kV and 100 mA (XRD, D/Max-IIIC, Rigaku, Tokyo, Japan), and the result is shown in Fig. S2 (supplementary material). Figures 4(a) and 4(b) show

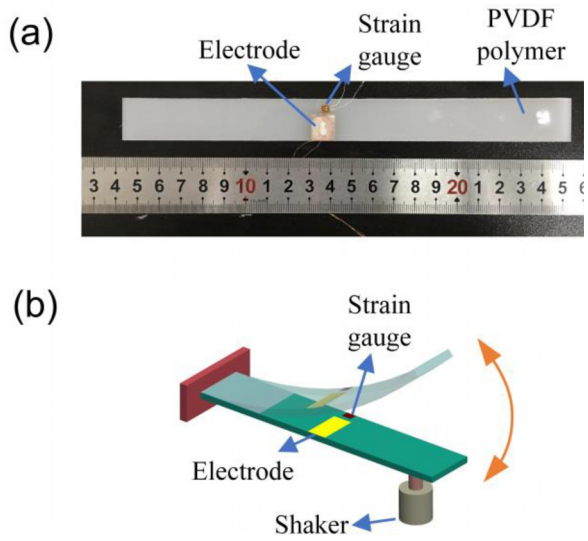

FIG. 3. (a) Photo of the PVDF sample. (b) The schematic view of the nonlinear flexoelectric measurement of the PVDF polymer.

the induced electric polarization as a function of the applied strain gradient in the BTS ceramic and PIN-PMN-PT single crystal. The results indicate that, with the increase in the strain gradient, the trend of the polarization will deviate from a straight line, showing an obvious nonlinear property. However, for the hard materials such as the BTS ceramic and the PIN-PMN-PT single crystal, the maximum strain gradient only reaches the level of 0.1 m^{-1}. Therefore, the nonlinearity was less remarkable compared with that in PVDF, where the strain gradient reaches as high as 1.75 m^{-1} [Fig. 4(c)]. All of these kinds of materials could be well fitted by using Eq. (8), demonstrating the linear behavior in the small strain gradient range while the nonlinear

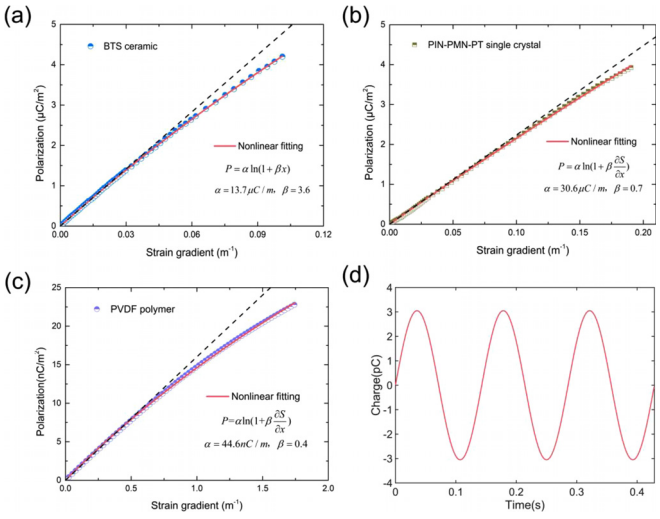

FIG. 4. (a)–(c) The relationship between the polarization and strain gradient in the BTS ceramic, PIN-PMN-PT single crystal, and PVDF polymer, respectively. (d) Bending-induced charge at a strain gradient of 1.75 m^{-1} for the PVDF polymer.

behavior is in the large strain gradient range. It can be seen that the nonlinear crossover occurs for BST, PIN-PMN-PT, and PVDF at strain gradients $1/3.6 = 0.28\ m^{-1}$, $1/0.7 = 1.43\ m^{-1}$, and $1/0.4 = 2.5\ m^{-1}$, respectively. It is worth underlining that the large strain gradient, especially for PVDF, may result in mechanical fracture or take nonlinear deformation, which brings distortions to the measured results. The real-time data of the PVDF polymer are shown in Fig. 4(d). Based on the ionic chain model and nonlinear expression, we can conclude that the effective flexoelectric coefficient of these materials can be expected to decrease to the nC/m level when the magnitude of the strain gradient reaches 10^6–$10^7\ m^{-1}$, whereby the discrepancy of flexoelectric coefficients in ferroelectric materials can be possibly resolved.

In summary, in this paper, the nonlinear property of the flexoelectricity was investigated from both the theoretical and experimental aspects. The ionic chain model predicts a strong nonlinearity of the flexoelectricity as the strain gradient increases to high orders of magnitude. This provides an explanation for the long-standing discrepancy between the flexoelectric coefficient of bulk and nanoscale dielectric materials. The results presented in this work indicate a declining flexoelectric coefficient as the strain gradient increases, matching with the previous reports about the thin film material.

See the supplementary material for the ion chain model of PVDF and the XRD pattern of the PVDF polymer.

This work was supported by the National Science Foundation of China (Nos. 11574126, 51605052, 51975065, and 51972157) and the Fundamental Research Funds for the Central Universities (No. 2019CDQYJX008). Financial support from the National Key Research and Development Plan of China under Grant No. 2017YFB0406300 is also acknowledged.

REFERENCES

[1]S. Sidhardh and M. C. Ray, Int. J. Mech. Mater. Des. **14**, 1–20 (2018).
[2]J. Narvaez, F. V. Sancho, and G. Catalan, Nature **538**, 219–221 (2016).
[3]X. T. Zhang, Q. Pan, D. X. Tian, W. F. Zhou, P. Chen, H. F. Zhang, and B. J. Chu, Phys. Rev. Lett. **121**, 057602 (2018).
[4]J. Liu, Y. Zhou, X. P. Hu, and B. J. Chu, Appl. Phys. Lett. **112**, 232901 (2018).
[5]A. Abdollahi, F. Vasquez-Sancho, and G. Catalan, Phys. Rev. Lett. **121**, 205502 (2018).
[6]H. Lu, C. W. Bark, D. E. Ojos, J. Alcala, C. B. Eom, G. Catalan, and A. Gruverman, Science **336**, 59 (2012).
[7]U. K. Bhaskar, N. Banerjee, A. Abdollahi, Z. Wang, D. G. Schlom, G. Rijnders, and G. Catalan, Nat. Nanotechnol. **11**, 263 (2016).
[8]L. Shu, W. Huang, S. Kwon, Z. Wang, F. Li, X. Wei, S. Zhang, M. Lanagan, X. Yao, and X. Jiang, Appl. Phys. Lett. **104**, 232902 (2014).
[9]L. Shu, M. Wan, Z. Wang, L. Wang, S. Lei, T. Wang, W. Huang, N. Zhou, and Y. Wang, Appl. Phys. Lett. **110**, 192903 (2017).
[10]G. Catalan, A. Lubk, A. H. G. Vlooswijk, E. Snoeck, C. Magen, A. Janssens, G. Rispens, G. Rijnders, D. H. A. Blank, and B. Noheda, Nat. Mater. **10**, 963 (2011).
[11]K. Chu, B. K. Jang, J. H. Sung, Y. A. Shin, E. S. Lee, K. Song, J. H. Lee, C. S. Woo, S. J. Kim, S. Y. Choi, T. Y. Koo *et al.*, Nat. Nanotechnol. **10**, 972 (2015).
[12]J. Narvaez and G. Catalan, Appl. Phys. Lett. **104**, 162903 (2014).
[13]L. Shu, R. Liang, Z. Rao, L. Fei, S. Ke, and Y. Wang, J. Adv. Ceram. **8**, 153 (2019).
[14]Q. Deng, L. P. Liu, and P. Sharma, J. Mech. Phys. Solids. **62**, 209–227 (2014).
[15]Y. Zhou, J. Liu, X. P. Hu, B. J. Chu, S. T. Chen, and D. Salem, IEEE. Trans. Dielectr. Electr. Insul. **24**, 727–731 (2017).
[16]S. M. Kogan, Sov. Phys. Solid State **5**, 2069 (1964).
[17]J. Narvaez, S. Saremi, J. W. Hong, M. Stengel, and G. Catalan, Phys. Rev. Lett. **115**, 037601 (2015).
[18]L. Shu, X. Wei, T. Pang, X. Yao, and C. Wang, J. Appl. Phys. **110**, 104106 (2011).
[19]H. Quang and Q. He, and Proc. R. Soc. London, Ser. A **467**, 2369 (2011).
[20]X. Wen, D. F. Li, K. Tan, Q. Deng, and S. P. Shen, Phys. Rev. Lett. **122**, 148001 (2019).
[21]H. Zhou, Y. M. Pei, J. W. Hong, and D. N. Fang, Appl. Phys. Lett. **108**, 101908 (2016).
[22]P. Zubko, G. Catalan, and A. K. Tagantsev, Annu. Rev. Mater. Res. **43**, 387 (2013).
[23]R. Maranganti and P. Sharma, Phys. Rev. B **80**, 054109 (2009).
[24]Q. Deng and S. P. Shen, Smart. Mater. Struct. **27**, 105001 (2018).
[25]G. Catalan, L. J. Sinnamon, and J. M. Gregg, J. Phys.: Condens. Matter **16**, 2253 (2004).
[26]P. Zubko, G. Catalan, A. Buckley, P. R. L. Welche, and J. F. Scott, Phys. Rev. Lett. **99**, 167601 (2007).
[27]D. Lee, A. Yoon, S. Y. Jang, J. G. Yoon, J. S. Chung, M. Kim, J. F. Scot, and T. W. Noh, Phys. Rev. Lett. **107**, 057602 (2011).
[28]S. Shen and S. Hu, J. Mech. Phys. Solids. **58**, 665 (2010).
[29]B. L. Wang, S. Y. Yang, and P. Sharma, Phys. Rev. B. **100**, 035438 (2019).
[30]A. H. Rahmati, S. Y. Yang, S. Bauer, and P. Sharma, Soft Matter **15**, 127–148 (2019).
[31]J. Y. Fu and L. E. Cross, Appl. Phys. Lett. **91**, 162903 (2007).
[32]J. Y. Fu, W. Zhu, N. Li, and L. E. Cross, J. Appl. Phys. **100**, 024112 (2006).
[33]B. C. Jeon, D. Lee, M. H. Lee, S. M. Yang, S. C. Chae, T. K. Song, D. B. Sang, S. C. Jin, G. Y. Jong, and T. W. Noh, Adv. Mater. **25**, 5643 (2013).
[34]W. Huang, S. R. Kwon, S. Zhang, F. G. Yuan, and X. Jiang, J. Intell. Mater. Syst. Struct. **25**, 271 (2014).
[35]B. Chu, W. Zhu, N. Li, and L. E. Cross, J. Appl. Phys. **106**, 104109 (2009).
[36]H. Zhang and B. Chu, J. Eur. Ceram. Soc. **38**, 2520–2525 (2018).
[37]L. Shu, X. Wei, L. Jin, Y. Li, H. Wang, and X. Yao, Appl. Phys. Lett. **102**, 152904 (2013).
[38]S. J. Huang, T. Kim, D. Hou, D. Cann, J. L. Jones, and X. N. Jiang, Appl. Phys. Lett. **110**, 222904 (2017).
[39]L. Shu, T. Li, Z. Wang, F. Li, L. Fei, Z. Rao, M. Ye, S. Ke, W. Huang, Y. Wang, and X. Yao, Appl. Phys. Lett. **111**, 162901 (2017).
[40]W. Ma and L. E. Cross, Appl. Phys. Lett. **81**, 3440 (2002).
[41]S. Kwon, W. Huang, L. Shu, F. G. Yuan, J. P. Maria, and X. Jiang, Appl. Phys. Lett. **105**, 142904 (2014).
[42]K. Chu and C. Yang, Phys. Rev. B. **96**, 104102 (2017).
[43]A. Abdollahi, C. Peco, D. Millán, M. Arroyo, G. Catalan, and I. Arias, Phys. Rev. B **92**, 094101 (2015).